Pressure-Induced Structural, Optical and Magnetic Modifications in Lanthanide SMMs

Fabrice Pointillart, Boris Le Guennic, Olivier Cador

Chemistry–A European Journal
Concept
doi.org/10.1002/chem.202400610
Chemistry Europe
European Chemical Societies Publishing
www.chemeurj.org

Pressure-Induced Structural, Optical and Magnetic Modifications in Lanthanide Single-Molecule Magnets

Fabrice Pointillart,*[a] Boris Le Guennic,[a] and Olivier Cador[a]

Lanthanide Single-Molecule Magnets are fascinating objects that break magnetic performance records with observable magnetic bistability at the boiling temperature of liquid nitrogen, paving the way for potential applications in high-density data storage. The switching of lanthanide SMM has been successfully achieved using several external stimuli such as redox reaction, pH titration, light irradiation or solvation/desolvation thanks to the high sensitivity of the magnetic anisotropy to any structural change in the lanthanide surrounding. Nevertheless, the use of applied high pressure as an external stimulus is largely underused, especially considering that it can be combined with high pressure X-ray diffraction to establish a complementary structure-property relationship. This Concept article summarizes the few relevant examples of investigations of lanthanide SMMs under applied high pressure, provides conclusions on the effect of such stimulus on molecular structures and magnetic anisotropy, and finally draws perspective on the future development of magnetic measurements under applied pressure.

Introduction

Lanthanide ions are intensely studied because of their particular magnetic characteristics (high magnetic moment and strong magnetic anisotropy) and their specific luminescence. The latter is easily recognizable with the line-shape emission bands ranging from the visible to near-infrared spectroscopic spectrum. Such optical properties open applications for instance in the elaboration of OLEDs,[1] bioimaging sensors,[2] time-resolved luminescent immunoassays[3] or imaging microscopy.[4] The former were exploited in the conception of Single-Molecule Magnets (SMMs)[5] having potential applications in high density magnetic data storage due to their magnetic bistability.[6] SMMs could be also suitable candidates for other applications such as quantum computing[7] and spintronics.[8] Especially, the use of lanthanide ions in the SMM design has enabled us to determine the highest performance currently available, with the observation of magnetic memory close to the boiling point of liquid nitrogen for high axial dysprosocenium cations[9] and their derivatives,[10] divalent terbium metallocene[11] and mixed-valence dysprosium dimer.[12] Since the first discovery of slow magnetic relaxation for a lanthanide mononuclear complex,[13] the level of understanding of their magnetic behavior has been improved thanks to structure-properties relationship investigations demonstrating the predominant role of the crystal field effect/electronic distribution on the magnetic anisotropy[14] as well as the matrix nature and molecular vibrations[15] on the magnetic relaxation rate. Such studies highlighted the high sensitivity of the lanthanide magnetism to any structural changes making them ideal candidates for designing molecular switches. As recently reviewed, the SMM behavior switching can be achieved using redox reaction, pH variation, solvation/desolvation process or light irradiation.[16] The application of pressure is a promising alternative stimulus to those mentioned above for inducing a switch in magnetic behavior. The monitoring of structural modifications under high pressure for molecular systems, thanks to the advances in pressure cell technology,[17] is one of the major recent advances that allows magneto-structural correlations. High pressure was already used to induce polymerization,[18] color change[19] and solvation/desolvation,[20] to switch molecular conductivity,[21] spin-crossover behavior,[22] magnetic ordering temperature for organic[23] and coordination complexes[24] or even to tune the photomagnetic response.[25] Among these pressure-induced magnetic behaviors, the spin crossover phenomenon was undoubtedly the most studied and has called upon a plethora of under-pressure characterization techniques. Indeed, pressure induced spin crossover has been monitored by magnetic susceptibility measurements thanks to clamp-type piston-cylinder pressure cell,[26] in multiferroics by Raman spectroscopy,[27] in Perovskite by synchrotron powder X-ray diffraction[28] and in metal-organic framework by ^{57}Fe Mössbauer.[29] Optical properties has also been monitored under applied pressure in absorption[30] and emission[31] in coordination compounds.

To focus on SMM switching,[32] high pressure was mainly applied on manganese-based SMMs[33] to modulate their magnetic performances. All the previously mentioned switching physical properties on the high-pressure effect were carried out on transition metal compounds while similar experiments on lanthanide molecular systems are very rare.

The present Concept article aims to review the few main examples of magnetic and X-ray diffraction investigations of lanthanide SMMs under applied pressure. After general con-

[a] Dr. F. Pointillart, Dr. B. Le Guennic, Prof. O. Cador
Univ Rennes, CNRS, ISCR (Institut des Sciences Chimiques de Rennes) – UMR 6226 35000 Rennes (France)
E-mail: fabrice.pointillart@univ-rennes.fr

clusions about the knowledges acquired from such experiments, we suggested perspective directions to develop this challenging research field which is still in its infancy.

Results and Discussion

The first work of applied pressure on lanthanide SMM discussed in this review is an ab initio computational study.[34] Indeed this approach has already demonstrated is effectiveness in describing and understanding both structural and electronic properties.[35] The aim of this work was to be able to control the direction of the anisotropy axis by applying pressure. To do so, the authors selected the {Na[Dy(DOTA)(H_2O)]·4H_2O} (**1**) (H_4DOTA = 1,4,7,10-tetraazacyclododecane-1,4,7,10-N,N′,N″,N‴-tetraacetic acid) complex based on their previous calculations which showed that the first excited Kramers doublet (KD) is close in energy to the ground KD with magnetic anisotropy axis perpendicular to the one of the ground state.[36] Their results demonstrated that by applying pressure to lanthanide molecular magnetic systems, detectable changes in magnetic anisotropies could be achieved, such as the rotation of the magnetic anisotropy axis direction.

Nevertheless, contrary to what was expected, the rotation of the apical water molecule has negligible effect on the magnetic anisotropy while both crystal field strength i.e. modulation of the Dy–O distances under applied pressure and Madelung potential played a major role.

In 2019, J. Overgaard and coll.[37] reported the first quantitative experimental investigation of applied pressure effect on lanthanide SMM. The target systems were mononuclear complexes of Dy(III) (**2**)[38] and Ho(III) (**3**)[39] with formula [(^{t}BuPO(NH^{i}Pr)$_2$)$_2$Ln(H_2O)$_5$][I]$_3$·(^{t}BuPO(NH^{i}Pr)$_2$)$_2$·(H_2O) which crystallized in the centrosymmetric triclinic space group P-1. The Ln(III) center adopted a pseudo-D_{5h} symmetry with five water molecules coordinated in equatorial positions while the two axial positions are occupied by two phosphonic diamide ligands. The single-crystal X-ray diffraction study under applied pressure demonstrated that the two analogues undergo two phase transitions at 0.5 GPa and 1.4 GPa. Between these two pressures the systems crystallized in monoclinic space group I2/a while for pressure higher than 1.4 GPa the crystallization takes place in monoclinic space group $P2_1/c$. The existence of phase transitions prevented any comparison of the cell parameters when gradually applying pressure. Nevertheless, the most important point for interpreting the magnetic behavior remains the local environment of the lanthanide center. In this respect, the degree of deformation of the D_{5h} symmetry polyhedron increased with increasing pressure. At ambient pressure, **2** displayed a magnetic bistability with steps in the hysteresis loops in the 4–12 K temperature range indicating fast relaxation Quantum Tunneling of Magnetization (QTM). Applying pressure at fixed temperatures of 4 K, 8 K and 12 K induced hysteresis loops getting narrower with a raise of the step intensities close to 0 Oe indicating a more efficient QTM. Ab initio calculations revealed significant variations in the energy barrier in relation to the modulation of the Ln–O distances and the axial O–Ln–O angle. Finally, on the basis of their computational study, the authors suggested that intermolecular interactions (Madelung constants) may play a predominant role in the variations of electronic energy levels which is in agreement with what was theoretically proposed for **1**.

Fabrice Pointillart obtained his PhD in physics and chemistry of materials from Pierre et Marie Curie University in 2005, supervised by Prof. Cyrille Train and Prof. Michel Verdaguer. After a postdoctoral research at the University of Florence with Prof. Roberta Sessoli he joined the University of Rennes in 2007, as a CNRS researcher. He is actually CNRS Research Director and head leader of the Molecular Multifunctional Materials group. His current research interests are focused on multifunctional molecular materials based on lanthanides combining magnetic and (chir)optical properties for the observation of single molecule magnet behavior, magneto-chiral dichroism and circularly polarized luminescence.

Boris Le Guennic received his Ph.D. in Chemistry from the University of Rennes in 2002. He then successively moved to the Universities of Erlangen, Buffalo, and Bonn for postdoctoral stays in the groups of Profs. Jochen Autschbach and Markus Reiher. In 2005, he was appointed as CNRS researcher at ENS de Lyon (France). In 2011, he moved to the Chemical Sciences Institute of Rennes (University of Rennes, France) where he is currently Senior CNRS researcher. He is the head of the Inorganic Theoretical Chemistry Team since 2018. His research is devoted mainly to the application of quantum chemical methodologies for the interpretation of magnetic and (chir-)optical properties in transition metal and f-element complexes, with a particular emphasis on lanthanide-based Single Molecule Magnets.

The research activities of Olivier Cador started in 1994 in Bordeaux (France). From its beginnings he contributes to the development of molecular magnetism under different aspects. He mainly focused on the studies of the magnetic properties of systems with various dimensionalities, from nanoparticles to isolated molecules which show quantum behaviors, and finally to magnets with atypical behaviors. Since he has been recruited by Université de Rennes 1 in 2003 its researches are oriented toward multifunctional molecular-based materials. He oriented part of its activities on Single-Molecule Magnets (SMMs); more particularly those based on lanthanides. He is full Professor at Université de Rennes 1 since 2017.

Phase transition induced by applied pressure is often observed as attested by another study done again by J. Overgaard on the five-coordinated unsolvated [Dy(Mes*O)$_2$(THF)$_2$Br] (**4**) SMM (Mes* = 2,4,6-tri-tert-butylpenhyl) (Figure 1a).[40]

The latter crystallized in the triclinic space group P-1 with a Dy(III) center in a distorted trigonal bipyramidal geometry formed by the two anionic aryloxide ligands (Mes*O), two THF molecules and one bromide. The phase transition was identified for pressure weaker than 0.08 GPa as well as for T inferior to 258 K. The high-pressure single-crystal X-ray diffraction was investigated up to 2.92 GPa with an initial pressure of 0.08 GPa. All the unit cell lengths decreased as expected, with a 17% reduction in cell volume at 2.92 GPa compared with the initial pressure (Figure 1b). More interesting was the distortion of the coordination sphere around the Dy(III) ion induced by the applied pressure and evaluated by the SHAPE program.[41] In fact, the phase transition led to a change of surrounding symmetry from C_{4v} to D_{3h} while between 0.08 GPa and the highest pressure, no significant variation in bond length, angle and symmetry was observed. The computational investigation confirmed that the nature, energy and composition of the KD did not change under pressure. Similar conclusions were drawn for the magnetic anisotropy and dipolar interaction. Nevertheless, measurable broadening in the hysteresis loops were observed with opening values at 5 kOe increasing from 2.11 kOe at 0 GPa to 3.61 kOe at 1.11 GPa. The authors pointed out the difficulties to measure the ac frequency dependence of the magnetic susceptibility due to the BeCu out-of-phase background ac signal. Indeed, as the BeCu pressure cell is conductive, it generated eddy currents leading to a strong temperature independent but frequency dependent in-phase and out-of-phase AC signal. Thus the AC signal collected at 25 K for the BeCu pressure cell was subtracted from the corresponding data of the investigated sample leading to clean χ_M' and χ_M'' signals of the sample. Nevertheless such treatment is suitable for frequencies $<$500 Hz because at higher frequencies, eddy currents become too large and the AC signal becomes too distorted to be exploited.[42] The pressure dependence of the relaxation time in the 18–44 K temperature range was established demonstrating a pressure-independent behavior of the Raman process for **4**. Since no significant variation in the bond lengths of the first coordination sphere was observed under applied pressure, no significant modification of the Orbach process was expected. The slight broadening in the hysteresis loop at non-zero magnetic fields could be due to the partial cancellation of the QTM induced by intermolecular dipolar interactions. Indeed, the applied pressure slightly modifies the Dy–Dy distance that might influence the dipolar interactions.

In the same year, J. Overgaard in collaboration with a research group at the University of Manchester reported another experimental and theoretical study of the pressure dependence of structural and magnetic behavior.[43] This investigation was carried out on the dysprocenium complex of formula [Dy(Cp^{ttt})$_2$][B(C$_6$F$_5$)$_4$] (**5**) (Cp^{ttt} = 1,2,4-tri(tert-butyl)cyclopentadienide) (Figure 2a) which is one of the best performing SMM reported to date.[9a] High-pressure crystallography revealed significant intramolecular distortions with increasing pressure. Indeed, the distance between the centroid of the Cp^{ttt} and the Dysprosium center decreases from 2.32(1) Å (at 0 GPa) to 2.26(7) Å (at 3.52 GPa) with rings more planar. Concomitantly the dysprosium moved away from the molecular center. These two structural distortions were expected to have an opposite effect on the magnetic axiality of **5**. Magnetic measurements at ambient pressure exhibited an open hysteresis loop up to 66 K at zero field and a sweep rate of 22 Oe s^{-1}.

The combination of direct current magnetization decay and alternating current magnetic susceptibility measurements led to the thermal dependence plot of the relaxation time. The best fit demonstrated that Orbach, Raman and QTM regimes are dominating for T $>$ 60 K, intermediate temperature and T $<$ 10 K, respectively. Similar magnetic investigations were carried out under applied pressure. At 1 GPa and high temperature (Orbach regime), hysteresis loop measurements showed no significant change while at low temperature, the loss of magnetization is consistent with an increase of the QTM and/or Raman relaxation rate. To confirm this trend, the authors fitted the thermal dependence of τ from ambient pressure to 0.37 GPa highlighting a decrease in both Raman and QTM rates while for higher pressures, relaxations appeared to become faster (Figure 2b) as observed on hysteresis loops. Finally, the authors

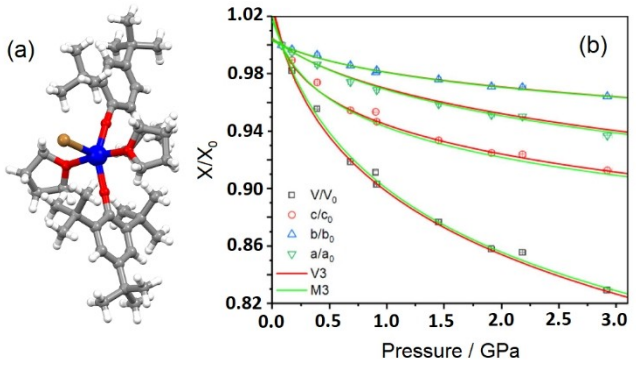

Figure 1. (a) Molecular structure of **4**. (b) The variation of the normalized unit cell parameters in the pressure range of 0.08-3 GPa. Adapted with permission from ref. [40]. Copyright 2023, American Chemical Society.

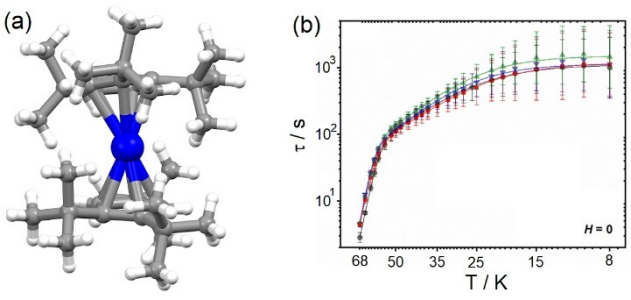

Figure 2. (a) Molecular structure of **5**. (b) Thermal variation of the relaxation time (τ) for **5** at ambient pressure (gray plots), 0.37 GPa (green plots), 0.79 GPa (blue plots) and 1.2 GPa (red plots) with the corresponding best fitted data at zero applied magnetic field. Adapted with permission from ref. [43]. Copyright 2023, Royal Society of Chemistry.

performed ab initio calculations to rationalize their observations. The electronic structure is unaffected by the pressurization from 0 to 1.01 GPa whereas for higher pressures, it was suggested that the relaxation occurred through the 5th KD (1250 cm^{-1}) at 1.5 GPa or the 4th (1125 cm^{-1}) at 3.08 GPa.

In 2017, M.-L. Tong and coll. reported the first bifunctional complex involving both piezochromism and SMM behavior.[44] To realize such a system, the aggregation-induced emission active ligand 2-methoxy-6-[[[4-(1,2,2-triphenylvinyl)phenyl]imino]-methyl]phenol (HTPEIP^{OMe}) was associated with a Dy(III) ion leading to the formation of a dinuclear compound of formula $[Dy_2(HTPEIP^{OMe})_2(OAc)_4(NO_3)_2]$ (**6**). Single-crystal X-ray diffraction study revealed that **6** crystallized in the triclinic P-1 space group. Each Dy(III) ion is coordinated to two HTPEIP^{OMe} ligands, four μ-OAc$^-$ anions and two chelating NO_3^-. The coordination sphere around the Dy(III) ion is nine-coordinated, surrounded by nine oxygen atoms and has adopted a distorted single-capped square-antiprismatic geometry. The initial color of the crystal is yellow and no change of color was observed after grinding. Nevertheless, under an applied pressure of 0.5 GPa, the crystalline sample turned orange while the initial color could be recovered after solvent fuming with acetonitrile vapor. The piezochromism phenomenon was confirmed by UV-visible diffuse reflectance and photoluminescence with a shift of the absorption band from 475 nm to 630 nm as well as a shift of the emission band from 593 nm to 603 nm. Thanks to the help of powder X-ray diffraction, the authors attributed the piezochromism to morphology transition from the crystalline state (ambient pressure) to amorphous state (under applied pressure).[45] Moreover **6** displayed a SMM behavior in zero applied magnetic field with slow magnetic relaxation occurring through a combination of QTM, Raman and Orbach processes. Upon applied pressure, no significant change was observed in the temperature regime of the Raman and Orbach processes while the maximum of the out-of-phase component of the magnetic susceptibility shifts to higher frequency at 2 K. Such observation indicated a modulation of the QTM rate under applied pressure.

The second example of piezochromic SMM was reported in 2023 by our research team.[42] The investigation was carried out on the well-known $[^{162}Dy(tta)_3(L)]\cdot C_6H_{14}$ (**7**) (tta$^-$ = 2-thenoyltrifluoroacetonate and L = 4,5-bis(propylthio)-tetrathiafulvalene-2-(2-pyridyl)benzimidazole-methyl-2-pyridine)) complex for which structural, magnetic and isotopic enrichment studies were already reported.[45] One of the original aspects of this work is the use of pure ^{162}Dy isotope as metal center. Indeed such dysprosium isotope possesses a zero nuclear spin (I = 0) prohibiting any hyperfine coupling between electronic and nuclear spins. The ambient pressure X-ray structure revealed the formation of a mononuclear coordination complex in which the Dy(III) ion is surrounded by one L ligand and three tta$^-$ ancillary ligands leading to a N_2O_6 coordination sphere with a D_{4d} square antiprism symmetry with a deviation of 0.54 from the ideal symmetry (SHAPE analysis).[35]

Cell volume compression is close to 20% at 2.43 GPa with the a and b axes being the most affected. A look at the first coordination sphere of the metal center reveals inhomogeneous deformation of the eight Dy–X distances, four of which are compressed (3.3%) while the other four remain almost unchanged (0.2%). As a result, the deviation from the ideal D_{4d} symmetry increases from 0.54 to 0.65. Applying an external pressure increased the electron withdrawal effect due to the electrostatic interaction with the Dy(tta)$_3$ moiety, resulting in a decrease of the energy of the LUMO and hence a red shift of the corresponding Intra Ligand Charge Transfer (ILCT) and a reversible color change from orange (0 GPa) to purple (P > 1.17 GPa) (Figure 3c). The SMM behavior of **7** was previously investigated.[46] Pressurization preserved the slow magnetic relaxation but the frequency maximum at 2 K was shifted from 15 Hz (0 GPa) to 50 Hz (1.17 GPa) (Figure 3b). High pressure thermal dependence of the magnetic susceptibility measurements allowed the extraction of the relaxation time and the determination of the relaxation through a combination of QTM, Raman and Orbach processes. The increase of pressure led to a decrease of the effective energy barrier from 35 K (0 GPa) to 21 K (1.17 GPa) as well as an increase of the QTM efficiency from 0.0082 s (0 GPa) to 0.0034 s (1.17 GPa). Both trends are in agreement with the distortion of the coordination sphere around the Dy(III) center. The pressure effect on the dynamic magnetic properties was found reversible (Figure 3b). . External pressure tended to close the butterfly hysteresis loop in field at 2 K with an opening of 650 Oe for 0 GPa and 400 Oe for 1.17 GPa at 1000 Oe (Figure 3c) due to the increase of efficiency of the under-energy barrier relaxation processes. Playing with a pure isotopologue ruled out the role of the hyperfine coupling in the existence of QTM, but the later may also be due to both

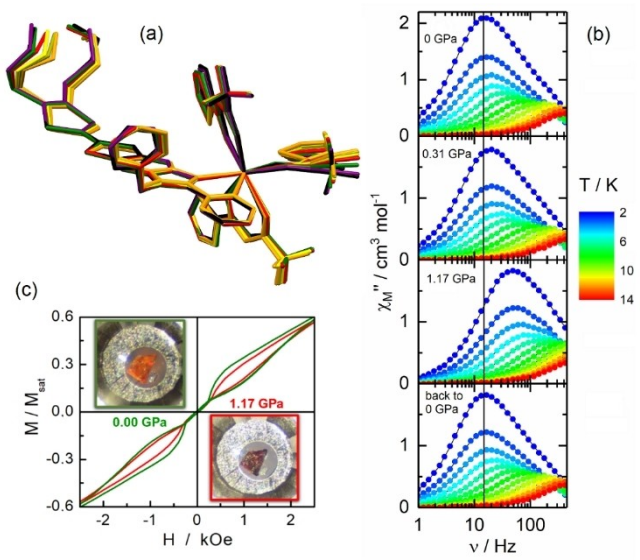

Figure 3. (a) single crystal X-ray structure of **7** recorded in the pressure range 0–2.43 GPa: P = 0 GPa (black), P = 0.22 GPa (purple), P = 0.46 GPa (green), P = 1.17 GPa (red), P = 1.63 GPa (yellow), P = 2.10 GPa (yellowish) and P = 2.43 GPa (orange). (b) Frequency dependence of χ_M" in the temperature range 2–14 K for 7 under P = 0 GPa, P = 0.31 GPa, P = 1.17 GPa and back to P = 0 GPa in zero applied magnetic field. The full vertical line is guide to the eye only. (c) Magnetic hysteresis loops at 2 K and a sweep rate of 16 Oe s^{-1} for **7** at 0 GPa (green) and 1.17 GPa (red) with the single crystal of **7** in the crystallographic pressure cell at the corresponding pressure values. Adapted with permission from ref. [42]. Copyright 2023, Wiley-VCH Verlag GmbH & Co. KGaA Weinheim.

intra- and intermolecular origins.[43,46f] We therefore decided to investigate the high pressure dc magnetic properties of the diluted $[^{162}Dy_{0.05}Y_{0.95}(tta)_3(L)]\cdot C_6H_{14}$ (**7@Y**) isotopologue. The variation in the opening of the hysteresis loop for **7@Y** is mainly related to the intramolecular structural modification induced by the applied pressure, since both hyperfine and dipolar interactions are cancelled. For low applied pressures ($P < 0.55$ GPa) the opening at 600 Oe increases from 450 Oe (0 GPa) to 590 Oe while it decreases for stronger pressures (520 Oe at 1.04 GPa). Ab initio calculations rationalized this behavior by applying a weak pressure evidencing the enhancement of the axiality of the GS and of the energy barrier. On the contrary, at higher pressures, the value of the energy barrier decreases from 98.8 cm^{-1} at ambient pressure to 40.2 cm^{-1} at 3 GPa and the transverse components of the g factor increase, favoring QTM efficiency. In conclusion the degradation in magnetic performance under applied pressure is due to the decrease of the Orbach efficiency in favor of under-barrier processes and the combination of magnetic investigations of **7** and **7@Y** has led to the conclusion that magnetic modulation under pressure has both intermolecular dipolar and intramolecular structural origins. Finally, we could imagine using the reversible piezochromism phenomenon as a sensor for pressure magnetic modulation.

Summary and Outlook

As demonstrated in this Concept article, lanthanide complexes that act as SMMs are suitable for studies under high pressure. In particular, their single crystal X-ray diffraction and slow magnetic relaxation can be monitored as a function of applied pressure. Moreover, the modulation of physical properties performances can be streamlined by computational approaches. Although a very limited number of studies have been undertaken so far, initial conclusions can be expressed to underline the potential of such measurements with lanthanide SMMs.

- High applied isostatic pressure (up to 3.6 GPa) is able to induce significant structural changes, which can be monitored by single-crystal X-ray diffraction study. Structural deformations are not homogeneous and strongly depend on the nature of chemical bonds and intermolecular contacts in the crystal structure.
- Ab initio calculations can be performed in tandem with (periodic) DFT optimization to rationalize or even predict structural deformations and their impact on physical properties such as magnetic behavior.
- Structural distortions and variations in electronic distribution due to the applied pressure are sufficiently strong to induce some magnetic anisotropy switching, leading to a deterioration in magnetic performance. The latter is due to an increase in the efficiency of under-barrier relaxation processes. The most affected magnetic relaxation process is the QTM due to its sensitivity to any transverse component of the magnetic anisotropy tensor.
- Discrimination between the intra- (distortion of the coordination sphere) and inter-molecular (dipolar interaction and interaction with the matrix) origins of the pressure-magnetic modulation can be established by studying the nuclear spin free metal isotope ($I = 0$) and its magnetic dilution. For the studied compounds, both origins contributed to the magnetic modulation, with a more preponderant effect for structural changes in crystal packing.
- A piezochromic effect was observed for lanthanide SMMs involving a ligand whose absorption transition lies in the visible spectrum, for instance a push-pull ligand. These molecular systems could therefore be used as optical sensors of magnetic performance.
- When probed, the reversibility of magnetic and optical switching when pressure is released was observed.

Given that the field of pressure-magnetic switching is still in its infancy, investigations and technical improvements are required to develop and understand it.

- The effect of pressure on the magnetic relaxation of lanthanide complexes is limited to a single metal ion (mainly dysprosium) but the exploration of a complete series of complexes involving several lanthanides would be useful to elaborate a magneto-structural correlation and rationalize the pressure effect as a function of the oblate/prolate and Kramers/non-Kramers character of the metal center.
- High pressure single-crystal X-ray diffraction experiments should be carried out at low temperature to establish optimum magneto-structural correlation, as slow magnetic relaxation is often observed at cryogenic temperatures.
- Increasing the applied pressure values accessible for non-synchrotron X-ray diffraction and magnetometry measurements is crucial to improving magnetic switching since the significant effect on electronic properties is expected for $P > 5$ GPa as shown by calculations.
- The pressure cell matter and design need to be improved to enable AC magnetic measurements at higher frequencies than 500 Hz while a transparency pressure cell would open the route to possible photo-magnetism such as pressure photo-induced spin crossover and single-molecule magnet.
- The most challenging part would be to control the effect of pressure on magnetic performance. To do so, the isostatic pressure applied has to be replaced by a uniaxial pressure along a selected axis or at least non-isostatic pressure. By applying such a pressure to an oriented single crystal, it might be possible to increase the electrostatic interaction between the metal center and the ligands along the most negatively charged direction for oblate ions or the least negatively charged direction for prolate ions, leading to a systematic improvement in magnetic performance.

Acknowledgements

The University of Rennes and The European Research Council (ERC) are acknowledged for financial support through the European Union's Horizon 2020 research and innovation

program (ERC-CoG MULTIPROSMM, grant agreement N°725184).

Conflict of Interests

The author declares no conflict of interest

Data Availability Statement

The data that support the findings of this study are available from the corresponding author upon reasonable request.

Keywords: Lanthanide · X-ray crystallography · High pressure · Single-Molecule Magnet · Piezochromism

[1] K. Kuriki, Y. Koike, Y. Okamoto, *Chem. Rev.* **2002**, *102*, 2347–2356.
[2] a) J.-C. G. Bünzli, *Chem. Rev.* **2010**, *110*, 2729–2755; b) R. M. Duke, E. B. Veale, F. M. Pfeffer, P. E. Kruger, T. Gunnlaugsson, *Chem. Soc. Rev.* **2010**, *39*, 3936–3953.
[3] E. G. Moore, A. P. S. Samuel, K. N. Raymond, *Acc. Chem. Res.* **2009**, *42*, 542–552 and references therein.
[4] A. Beeby, S. W. Botchway, I. M. Clarkson, S. Faulkner, A. M. Parker, D. Parker, J. A. G. Williams, *J. Photochem. Photobiol. B* **2000**, *57*, 83–89.
[5] D. N. Woodruff, R. E. P. Winpenny, R. A. Layfield, *Chem. Rev.* **2013**, *113*, 5110–5148.
[6] D. Gatteschi, R. Sessoli, J. Villain, *Molecular Nanomagnets*, Oxford University Press, **2006**.
[7] S. Thiele, F. Balestro, R. Ballou, S. Klyatskaya, M. Ruben, W. Wernsdorfer, *Science* **2014**, *344*, 1135–1138.
[8] K. S. Pedersen, A.-M. Ariciu, S. McAdams, H. Weihe, J. Bendix, F. Tuna, S. Piligkos, *J. Am. Chem. Soc.* **2016**, *138*, 5801–5804.
[9] a) C. A. P. Goodwin, F. Ortu, D. Reta, N. F. Chilton, D. P. Mills, *Nature* **2017**, *548*, 439–442; b) F.-S. Guo, B. M. Day, Y.-C. Chen, M.-L. Tong, A. Mansikkamäki, R. A. Layfield, *Science* **2018**, *362*, 1400–1403; c) F.-S. Guo, B. M. Day, Y.-C. Chen, M.-L. Tong, A. Mansikkamäki, R. A. Layfield, *Angew. Chem. Int. Ed.* **2017**, *56*, 11445–11449; d) F.-S. Guo, B. M. Day, Y. C. Chen, M. L. Tong, A. Mansikkamäki, R. A. Layfield, *Angew. Chem. Int. Ed.* **2020**, *59*, 18844–18849; e) K. R. McClain, C. A. Gould, K. Chakarawet, S. J. Teat, T. J. Groshens, J. R. Long, B. G. Harvey, *Chem. Sci.* **2018**, *9*, 8492–8503.
[10] a) P. Evans, D. Reta, G. F. S. Whitehead, N. F. Chilton, D. P. Mills, *J. Am. Chem. Soc.* **2019**, *141*, 19935–19940; b) F.-S. Guo, M. He, G.-Z. Huang, S. R. Giblin, D. Billington, F. W. Heinemann, M.-L. Tong, A. Mansikkamäki, R. A. Layfield, *Inorg. Chem.* **2022**, *61*, 6017–6025; c) J. C. Vanjak, B. O. Wilkins, V. Vieru, N. S. Bhuvanesh, J. H. Reibenspies, C. D. Martin, L. F. Chibotaru, M. Nippe, *J. Am. Chem. Soc.* **2022**, *144*, 17743–17747; A. Vincent, Y. L. Whyatt, N. F. Chilton, J. R. Long, *J. Am. Chem. Soc.* **2023**, *145*, 1572–1579.
[11] C. A. Gould, K. R. McClain, J. M. Yu, T. J. Groshens, F. Furche, B. G. Harvey, J. R. Long, *J. Am. Chem. Soc.* **2019**, *141*, 12967–12973.
[12] C. A. Gould, K. R. McClain, D. Reta, J. G. C. Kragskow, D. A. Marchiori, E. Lachman, E.-S. Choi, J. G. Analytis, R. D. Britt, N. F. Chilton, B. G. Harvey, J. R. Long, *Science* **2022**, *375*, 198–202.
[13] N. Ishikawa, M. Sugita, T. Ishikawa, S. Koshihara, Y. Kaizu, *J. Am. Chem. Soc.* **2003**, *125*, 8694–8695.
[14] J. D. Rinehart, J. R. Long, *Chem. Sci.* **2011**, *2*, 2078–2085.
[15] A. Mattioni, J. K. Staab, W. J. A. Blackmore, D. Reta, J. Iles-Smith, A. Nazir, N. F. Chilton, *Nat. Commun.* **2024**, *15*, 485–495.
[16] a) P. Zhang, M. Perfetti, M. Kern, P. P. Hallmen, L. Ungur, S. Lenz, M. R. Ringenberg, W. Frey, H. Stoll, G. Rauhut, J. van Slageren, *Chem. Sci.* **2018**, *9*, 1221–1230; b) B. S. Dolinar, S. Gomez-Coca, D. I. Alexandropoulos, K. R. Dunbar, *Chem. Commun.* **2017**, *53*, 2283–2286; c) C. M. Dickie, A. L. Laughlin, J. D. Wofford, N. S. Bhuvanesh, M. Nippe, *Chem. Sci.* **2017**, *8*, 8039–8049; d) Z. Liang, M. Damjanovic, M. Kamila, G. Cosquer, B. K. Breedlove, M. Enders, M. Yamashita, *Inorg. Chem.* **2017**, *56*, 6512–6521; e) K. Suzuki, R. Sato, N. Mizuno, *Chem. Sci.* **2013**, *4*, 596–600; f) J.-L. Liu, Y.-C. Chen, Y.-Z. Zheng, W.-Q. Lin, L. Ungur, W. Wernsdorfer, L. F. Chibotaru, M.-L. Tong, *Chem. Sci.* **2013**, *4*, 3310–3316; g) X. Zhang, V. Vieru, X. Feng, J.-L. Liu, Z. Zhang, B. Na, W. Shi, B.-W. Wag, A. K. Powell, L. F. Chibotaru, S. Gao, P. Cheng, J. R. Long, *Angew. Chem. Int. Ed.* **2015**, *54*, 9861–9865; *Angew. Chem.* **2015**, *127*, 9999–10003; h) J.-Y. Ge, L. Cui, J. Li, F. Yu, Y. Song, Y.-Q. Zhang, J.-L. Zuo, M. Kurmoo, *Inorg. Chem.* **2017**, *56*, 336–343; i) D. Pinkowicz, M. Ren, L.-M. Zheng, S. Sato, M. Hasegawa, M. Morimoto, M. Irie, B. K. Breedlove, G. Cosquer, K. Katoh, M. Yamashita, *Chem. Eur. J.* **2014**, *20*, 12502–11513; j) M. Hojorat, H. Al Sabea, L. Norel, K. Bernot, T. Roisnel, F. Gendron, B. Le Guennic, E. Trzop, E. Collet, J. R. Long, S. Rigaut, *J. Am. Chem. Soc.* **2020**, *142*, 931–936; k) H. Tian, J.-B. Su, S.-S. Bao, M. Kurmoo, X.-D. Huang, Y.-Q. Zhang, L.-M. Zheng, *Chem. Sci.* **2018**, *9*, 6424–6433; l) F. Pointillart, J. Flores Gonzalez, V. Montigaud, L. Tesi, V. Cherkasov, B. Le Guennic, O. Cador, L. Ouahab, R. Sessoli, V. Kuropatov, *Inorg. Chem. Front.* **2020**, *7*, 2322–2334.
[17] a) S. A. Moggach, D. R. Allan, S. Parsons, J. E. Warren, *J. Appl. Crystallogr.* **2008**, *41*, 249–251; b) G. Giriat, W. Wang, J. P. Attfield, A. D. Huxley, K. V. Kamenev, *Rev. Sci. Instrum.* **2010**, *81*, 073905; c) J. Binns, K. V. Kamenev, G. J. McIntyre, S. A. Moggach, S. Parsons, *IUCrJ* **2016**, *3*, 168–179.
[18] S. A. Moggach, K. W. Galloway, A. R. Lennie, P. Parois, N. Rowantree, E. K. Brechin, J. E. Warren, M. Murrie, S. Parsons, *CrystEngComm* **2009**, *11*, 2601–2604.
[19] K. W. Galloway, S. A. Moggach, P. Parois, A. R. Lennie, J. E. Warren, E. K. Brechin, R. D. Peacock, R. Valiente, J. González, F. Rodríguez, S. Parsons, M. Murrie, *CrystEngComm* **2010**, *12*, 2516–2519.
[20] A. Prescimone, J. Sanchez-Benitez, K. K. Kamenev, S. A. Moggach, J. E. Warren, A. R. Lennie, M. Murrie, S. Parsons, E. K. Brechin, *Dalton Trans.* **2010**, *39*, 113–123.
[21] a) H. Benjamin, J. G. Richardson, S. A. Moggach, S. Afanasjevs, L. Warren, M. R. Warren, D. R. Allan, C. A. Morrison, K. V. Kamenev, N. Robertson, *Phys. Chem. Chem. Phys.* **2020**, *22*, 6677–6689; b) M. Mito, M. Fujino, H. Deguchi, S. Takagi, W. Fujita, K. Awaga, *Polyhedron* **2005**, *24*, 2501–2504.
[22] a) P. Guionneau, E. Collet, *Piezo- and Photo-Crystallography Applied to Spin-Crossover Materials. In Spin-Crossover Materials: Properties and Applications*, 1st ed., Halcrow, M. A., Ed., John Wiley & Sons Ltd.: Oxford, UK, **2013**; pp. 507–526; b) A. B. Gaspar, G. Molnár, A. Rotaru, H. J. Shepherd, *Comptes Rendus Chim.* **2018**, *21*, 1095–1120; c) P. Gütlich, V. Ksenofontov, A. B. Gaspar, *Coord. Chem. Rev.* **2005**, *249*, 1811–1829; d) L. Stoleriu, P. Chakraborty, A. Hauser, C. Stancu, C. Enachescu, *Phys. Rev. B* **2011**, *84*, 134102.
[23] a) K. Thirunavukkuarasu, S. M. Winter, C. C. Beedle, A. E. Kovalev, R. T. Oakley, S. Hill, *Phys. Rev. B* **2015**, *91*, 014412; b) T. Tanaka, W. Fujita, K. Awaga, *Chem. Phys. Lett.* **2004**, *393*, 150–152.
[24] a) C. H. Woodall, G. A. Craig, A. Prescimone, M. Misek, J. Cano, J. Faus, M. R. Probert, S. Parsons, S. Moggach, J. Martínez-Lillo, M. Murrie, K. V. Kamenev, E. K. Brechin, *Nat. Commun.* **2016**, *7*, 13870; b) W. Kaneko, M. Mito, S. Kitagawa, M. Ohba, *Chem. Eur. J.* **2008**, *14*, 3481–3489; M. Ohba, W. Kaneko, S. Kitagawa, T. Maeda, M. Mito, *J. Am. Chem. Soc.* **2008**, *130*, 4475–4484.
[25] M. K. Peprah, D. VanGennep, P. A. Quintero, O. N. Risset, T. V. Brinzari, C. H. Li, M. F. Dumont, J. S. Xia, J. J. Hamlin, D. R. Talham, M. W. Meisel, *Polyhedron* **2017**, *123*, 323–327.
[26] A. B. Gaspar, G. Molnar, A. Rotaru, H. J. Shepherd, *C. R. Chim.* **2018**, *21*, 1095–1120.
[27] I. Lyubutin, S. Starchikov, I. Troyan, Y. Nikiforova, M. Lyubutina, A. Gavriliuk, *Molecules* **2020**, *25*, 3808–3825.
[28] Y. Tsujimoto, S. Nakano, N. Ishimatsu, M. Mizumaki, N. Kawamura, T. Kawakami, Y. Matsushita, K. Yamaura, *Sci. Rep.* **2016**, *6*, 36253–36262.
[29] B. Vatsha, R. Goliath, G. Hearne, *ChemPlusChem* **2021**, *86*, 82–86.
[30] I. Shirotani, Y. Inagaki, W. Utsumi, T. Yagi, *J. Mater. Chem.* **1991**, *1*, 1041–1043.
[31] A. Sussardi, C. L. Hobday, R. J. Marshall, R. S. Forgan, A. C. Jones, S. A. Moggach, *Angew. Chem. Int. Ed.* **2020**, *59*, 8118–8122.
[32] A. M. Thiel, E. Damgaard-Moller, J. Overgaard, *Inorg. Chem.* **2020**, *59*, 1682–1691.
[33] a) A. Prescimone, C. J. Milios, S. Moggach, J. E. Warren, A. R. Lennie, J. Sanchez-Benitez, K. Kamenev, R. Bircher, M. Murrie, S. Parsons, E. K. Brechin, *Angew. Chem. Int. Ed.* **2008**, *47*, 2828–2831; b) A. Prescimone, J. Sanchez-Benitez, K. V. Kamenev, S. A. Moggach, A. R. Lennie, J. E. Warren, M. Murrie, S. Parsons, E. K. Brechin, *Dalton Trans.* **2009**, *36*, 7390–7395; c) Y. Suzuki, Y. Takeda, K. Awaga, *Phys. Rev. B* **2003**, *67*, 132402; d) A. Sieber, R. Bircher, O. Waldmann, G. Carver, G. Chaboussant, H. Mutka, H.-U. Güdel, *Angew. Chem. Int. Ed.* **2005**, *44*, 4239–4242; *Angew. Chem.* **2005**, *117*, 4311–4314; e) R. Bircher, G. Chaboussant, C. Dobe, H.-U. Güdel, S. T. Ochsenbein, A. Sieber, O. Waldmann, *Adv. Funct. Mater.* **2006**, *16*, 209–220; f) A. Sieber, G. Chaboussant, R. Bircher, C.

Boskovic, H.-U. Güdel, *Phys. Rev. B* **2004**, *70*, 172413; g) A. Prescimone, C. J. Milios, J. Sanchez-Benitez, K. V. Kamenev, C. Loose, J. Kortus, S. Moggach, M. Murrie, J. E. Warren, A. R. Lennie, S. Parsons, E. K. Brechin, *Dalton Trans.* **2009**, 4858–4867.
[34] M. Briganti, F. Totti, *Dalton Trans.* **2021**, *50*, 10621–10628.
[35] a) A. Caneschi, D. Gatteschi, F. Totti, *Coord. Chem. Rev.* **2015**, *289–290*, 357–378; b) A. Castro-Alvarez, Y. Gil, L. Llanos, D. Aravena, *Inorg. Chem. Front.* **2020**, *7*, 2478–2486; c) D. Aravena, *J. Phys. Chem. Lett.* **2018**, *9*, 5327–5333; d) A. Swain, A. Sarkar, G. Rajaraman, *Chem. Asian J.* **2019**, *14*, 4056–4073; e) B. Yin, L. Luo, *Phys. Chem. Chem. Phys.* **2021**, *23*, 3093–3105; f) K. Kotrle, R. Herchel, *Inorg. Chem.* **2019**, *58*, 14046–14057; g) B. Yin, C.-C. Li, *Phys. Chem. Chem. Phys.* **2020**, *22*, 9923–9933.
[36] M. Briganti, G. Fernandez Garcia, J. Jung, R. Sessoli, B. Le Guennic, F. Totti, *Chem. Sci.* **2019**, *10*, 7233–7245.
[37] M. S. Norre, C. Gao, S. Dey, S. K. Gupta, A. Borah, R. Murugavel, G. Rajaraman, J. Overgaard, *Inorg. Chem.* **2020**, *59*, 717–729.
[38] S. K. Gupta, T. Rajeshkumar, G. Rajaraman, R. Murugavel, *Chem. Sci.* **2016**, *7*, 5181–5191.
[39] S. K. Gupta, T. Rajeshkumar, G. Rajaraman, R. Murugavel, *Dalton Trans.* **2018**, *47*, 357–366.
[40] V. S. Parmar, A. M. Thiel, M. S. Norre, J. Overgaard, *Cryst. Growth Des.* **2023**, *23*, 6410–6417.
[41] M. Llunell, D. Casanova, J. Cirera, P. Alemany, S. Alvarez, S. *SHAPE Program for the Stereochemical Analysis of Molecular Fragments by Means of Continuous Shape Measures and Associated Tools*; Departament de Quimica Fisica, Departament de Quimica Inorganica and Institut de Quimica Teorica i Computacional-Universitat de Barcelona: Barcelona, Spain.
[42] F. Pointillart, J. Flores Gonzalez, H. Douib, V. Montigaud, C. J. McMonagle, B. Le Guennic, O. Cador, D. Pinkowicz, M. R. Probert, *Chem. Eur. J.* **2023**, e202300445.
[43] V. S. Parmar, A. M. Thiel, R. Nabi, G. K. Gransbury, M. S. Norre, P. Evans, S. C. Corner, J. M. Skelton, N. F. Chilton, D. P. Mills, J. Overgaard, *Chem. Commun.* **2023**, *59*, 2656–2659.
[44] W.-B. Chen, Y.-C. Chen, J.-L. Liu, J.-H. Jia, L.-F. Wang, Q.-W. Li, M.-L. Tong, *Inorg. Chem.* **2017**, *56*, 8730–8734.
[45] a) Z. Chi, X. Zhang, B. Xu, X. Zhou, C. Ma, Y. Zhang, S. Liu, J. Xu, *Chem. Soc. Rev.* **2012**, *41*, 3878–3896; b) Z. Ma, Z. Wang, X. Meng, Z. Ma, Z. Xu, Y. Ma, X. Jia, *Angew. Chem. Int. Ed.* **2016**, *55*, 519–522; c) B. Xu, Z. Chi, X. Zhang, H. Li, C. Chen, S. Liu, Y. Zhang, J. Xu, *Chem. Commun.* **2011**, *47*, 11080–11082; d) Y.-X. Zhu, Z.-W. Wei, M. Pan, H.-P. Wang, J.-Y. Zhang, C.-Y. Su, *Dalton Trans.* **2016**, *45*, 943–950.
[46] a) T. T. da Cunha, J. Jung, M.-E. Boulon, G. Campo, F. Pointillart, C. L. M. Pereira, B. Le Guennic, O. Cador, K. Bernot, F. Pineider, S. Golhen, L. Ouahab, *J. Am. Chem. Soc.* **2013**, *135*, 16332–16335; b) J. Jung, T. T. da Cunha, B. Le Guennic, F. Pointillart, C. L. M. Pereira, J. Luzon, S. Golhen, O. Cador, O. Maury, L. Ouahab, *Eur. J. Inorg. Chem.* **2014**, 3888–3894; c) F. Pointillart, K. Bernot, S. Golhen, B. Le Guennic, T. Guizouarn, L. Ouahab, O. Cador, *Angew. Chem. Int. Ed.* **2015**, *54*, 1504–1507; d) L. Tesi, Z. Salman, I. Cimatti, F. Pointillart, K. Bernot, M. Mannini, R. Sessoli, *Chem. Commun.* **2018**, *54*, 7826–7829; e) G. Fernandez Garcia, V. Montigaud, L. Norel, O. Cador, B. Le Guennic, F. Totti, F. Pointillart, *Magnetochemistryy* **2019**, *5*, 46–59; f) J. Flores Gonzalez, F. Pointillart, O. Cador, *Inorg. Chem. Front.* **2019**, *6*, 1081–1086.

Manuscript received: February 14, 2024
Accepted manuscript online: March 21, 2024
Version of record online: April 12, 2024